Validation of the activity expansion method with ultrahigh pressure shock equations of state

Forrest J. Rogers* and David A. Young
Physics Department, Lawrence Livermore National Laboratory, P.O. Box 808, Livermore, California 94550
(Received 6 June 1997)

Laser shock experiments have recently been used to measure the equation of state (EOS) of matter in the ultrahigh pressure region between condensed matter and a weakly coupled plasma. Some ultrahigh pressure data from nuclear-generated shocks are also available. Matter at these conditions has proven very difficult to treat theoretically. The many-body activity expansion method (ACTEX) has been used for some time to calculate EOS and opacity data in this region, for use in modeling inertial confinement fusion and stellar interior plasmas. In the present work, we carry out a detailed comparison with the available experimental data in order to validate the method. The agreement is good, showing that ACTEX adequately describes strongly shocked matter. [S1063-651X(97)03211-X]

PACS number(s): 52.25.Kn, 62.50.+p, 05.70.Ce

I. INTRODUCTION

The last 40 years have seen major advances in experimental high-pressure physics. The generation of one-dimensional shocks in condensed matter using chemical explosives, gas guns, and nuclear explosives has produced states of matter ranging up to pressures of 4000 Mbar and temperatures of 500 eV (1 eV=11 605 K). Measurement techniques have been steadily refined so that accurate characterization of ultrahigh pressure states of matter can be obtained [1]. These advances have been complemented by the success of the diamond-anvil technique [2] for producing high static pressures now approaching 5 Mbar. Recently laser-driven shock techniques [3] have been used successfully to measure the equation of state (EOS) of deuterium and a number of other materials in regions not previously accessible to experiment. The performance of inertial confinement capsules containing hydrogen isotopes is critically dependent on the EOS. The EOS for mixtures of low-Z elements in the range accessed by the new laser experiments is also important input data required to model giant planets and late stages of stars that have entered the horizontal branch of the Hertzsprung-Russell diagram [4]. In these cases, experiment can serve as a useful guide, but the amount of data required to carry out model calculations can only be obtained from theoretical calculations.

The properties of matter at high compression and high temperature present a challenge to theory, because the excited electronic states occur in condensed matter, not in isolated atoms or molecules. This requires a full self-consistent quantum-mechanical treatment of the electrons, including the occupation of excited states. For shock compressions of normal-density solids that attain temperatures of at most 1–2 eV the appropriate starting point is the zero-temperature electron band-structure calculation. The higher-temperature data now becoming available are in an intermediate regime between that of a solid and a partially ionized plasma having identifiable ions. Any successful model of shocked matter needs to pass smoothly between these extreme states of matter. Phenomena such as electron band crossings, charge transfer, electron shell ionization, and phase transitions all may occur in hot dense matter. The question of how, or even if, the bound states in a dense plasma are shifted by screening remains an unresolved experimental problem [5,6]. The problems associated with dense, high-temperature matter have not been solved in a comprehensive way.

A partial solution of the ultrahigh pressure equation of state can be found in the activity expansion method (ACTEX), which approximates the quantum-mechanical partition function of a mixture of atoms, ions, and electrons. It is exact in the weakly coupled plasma limit of high temperature, but becomes progressively less accurate as the condensed-matter regime is approached. It is useful because it overlaps the highest pressures reached in shock experiments, and a rigorous test of the theory is now possible. The theory underlying the ACTEX method has been developed over a number of years and is described in detail elsewhere [7–11]. It has been used extensively in astrophysical modeling and has been found to be in better agreement with helioseismic observations than other methods [12]. These data present an opportunity to directly compare ACTEX with experiments that test its limits of validity. A brief summary of the ACTEX method is given in Sec. II. Section III discusses the experimental data used to make comparisons. Section IV shows the comparison of theory with shock data. Section V concludes with a discussion.

II. THE ACTEX METHOD

The EOS of partially ionized plasmas has been of interest since the 1920s when Saha [13] introduced a method to include ionization equilibrium in weakly coupled stellar plasmas. This simple approach led to a breakthrough in stellar modeling and greatly increased our understanding of stars. Since that time there have been a number of attempts to improve on the method by adding plasma screening effects on bound states and nonideal Coulomb coupling corrections, in many cases using phenomenological reasoning [14–19]. The most fundamental approaches have been mainly concerned with obtaining terms through order $n^{5/2}$ in hydrogen plasmas [20–27], where $n=N/V$ is the number density.

*Electronic address: rogers4@llnl.gov

ACTEX is a systematic attempt to obtain similar results valid for higher-Z plasmas, where strong coupling exists between highly ionized ions. The philosophy behind the ACTEX approach is to sacrifice some degree of rigor in order to obtain reliable results over a wide range of mass density ρ, temperature T, and atomic number Z.

Fully quantum-mechanical activity expansion calculations are very complicated and, for practical calculations, limited to a few low-order terms [22–24]. However, in many regimes of interest the quantum mechanics only enters through degeneracy-weighted Boltzmann factors that control the ionization balance, while the Coulomb interaction terms are highly classical, e.g., at low density, the Saha equation with Debye-Hückel Coulomb corrections [28]. With these factors in mind it is possible to first work out global classical equations that describe partially ionized, arbitrarily coupled plasmas [8,9]. Then at a later stage of the analysis, after the underlying structure has been determined, classical electron-ion Boltzmann factors can be replaced with Tr $\exp(-\beta H)$ of the screened potential. In the static limit this is the Debye-Huckel (Yukawa) potential,

$$u_s = -\frac{\zeta_j e^2 e^{-r/\lambda_D}}{r}, \tag{1}$$

where ζ_j is the net ionic charge and

$$\lambda_D = \left(\frac{kT}{4\pi e^2 \Sigma_j n_j \zeta_j^2} \right)^{1/2} \tag{2}$$

is the Debye length. This results in an expansion that gives statically screened bound states and the lowest-order quantum corrections to the Coulomb interaction terms. In a few cases some higher-order quantum corrections are available from other sources and have been added. It is possible to further improve these results by using the Cooper-DeWitt formalism [29] to introduce electron degeneracy corrections into the screening length and directly into the Coulomb coupling terms. The major steps involved in the method are described in the following paragraphs.

The classical activity expansion of the grand canonical partition function (GCPF) of strongly coupled, fully ionized plasmas involves a many-body analysis of a very large number of both singly connected and multiply connected diagrams [30]. In contrast, only the multiply connected diagrams contribute to a density expansion of the canonical partition function. Abe [31] showed how to carry out an all-orders expansion in the density. The leading terms in the resulting convergent multicomponent expression for the nonideal Helmholtz free energy are

$$\frac{F - F_0}{VkT} = S_R + \sum_{ij} S_{ij} + \sum_{ijk} S_{ijk} + \cdots, \tag{3}$$

where

$$S_R = \frac{1}{12\pi \lambda_D^3}, \tag{4}$$

$$S_{ij} = -n_i n_j \left[B_{ij}(T, \lambda_D) + 2\pi \int_0^\infty \left(\beta u_{ij} - \frac{\beta u_{ij}}{2} \right) r^2 dr \right], \tag{5}$$

and $B_{ij}(T, \lambda_D)$ is the second virial coefficient for the static screened potential $u_{ij} = \zeta_i \zeta_j e^2 \exp(-r/\lambda_D)/r$. The S_{ijk} and higher-order terms systematically replace the divergent Coulomb virial coefficients with the virial coefficients for the Debye-Hückel potential [Eq. (1)]. The terms through order n^2, given by Eqs. (3)–(5), show that there are some differences in detail with the virial expansion of the screened Coulomb potential. For example, there appears a term of order $n^{3/2}$, i.e., the Debye-Hückel Coulomb interaction term, coming from the ring diagrams, while terms of order βu_{ij} and $(\beta u_{ij})^2$ are missing from the screened second virial coefficient. In the special case of the one-component plasma (OCP), much studied with Monte Carlo simulations [32], the Abe method recovers the strong-coupling limit [9]. Rogers and DeWitt [7] showed that the equivalent result in the grand canonical ensemble, including all singly and multiply connected diagrams, could be generated from the Abe density expansion. In the classical case this removes the complications related to the long-range Coulomb interaction and the multiply connected diagrams. However, due to the inversion technique, this expression is still not in proper form to study ionization balance; i.e., it is expressed in terms closely resembling the virial coefficients of the screened Coulomb potential, not cluster coefficients as would be expected for the GCPF. This is remedied by recollecting the virial-like terms to obtain an activity expression in terms of Mayer cluster coefficients of the statically screened Coulomb potential [8]. The next step is to everywhere replace classical Boltzmann factors $\exp(-\beta u)$ with Tr $\exp(-\beta H)$. These steps give an activity expansion of the GCPF in which the short-ranged classical divergences have been removed with quantum mechanics and the long-ranged divergences with convergent many-body resummations. This result is finally in a suitable form to allow the study of partially ionized plasmas. The bound states in the reorganized activity expression are screened by a static potential that has the Debye-Hückel (Yukawa) form Eq. (1), but the screening length,

$$\lambda_A = \left(\frac{kT}{4\pi e^2 \Sigma_j z_j \zeta_j^2} \right)^{1/2}, \tag{6}$$

is now dependent on the activity,

$$z_j = (2s_j + 1) \lambda\!\!\!^{-3}_j e^{u_j/kT}, \tag{7}$$

rather than the density, where

$$\lambda\!\!\!^{-}_j = \left(\frac{2\pi\hbar^2}{m_j kT} \right)^{1/2} \tag{8}$$

is the thermal de Broglie wavelength. It approaches the ion-sphere radius, $a = (3/4\pi n)^{1/3}$, at strong coupling, while the Debye length that appears in the density expansion, as is well known, becomes much less than a. These results are still only appropriate for fully ionized plasmas. The dynamic screening corrections, which are being neglected here, affect the bound state energies and also the Coulomb coupling

terms of low-Z plasmas [21]. However, the effects on the EOS are not large when $\lambda > \lambda_D$ [24].

Next, analogous to the way dissociation is treated in short-ranged molecular dissociation in low-density gases, an augmented set of activity variables is introduced to account for the formation of ions, atoms, and molecules [30]. These new variables are built from products of the fundamental particle activities and the Boltzmann factors that control the ionization balance between states of charge ζ_j and ζ_{j+1}.

The resulting activity expansion for the pressure that originally was expressed in terms of the basic components, i.e., electrons ''e'' and nuclei ''$\{i\}$'', is replaced with an expression that involves additional activity variables ''$\{i_c\}$'' that account for the possible composite particles (ions, atoms, molecules) that can form. Since the ACTEX analysis works from equations that include all possible interactions among the basic constituents of the system, plasma screening effects on bound states are automatically included. The static screening approximation limits the calculations to conditions such that $\lambda < \lambda_A$. The reorganized expansion has two noteworthy features: (1) it systematically pulls out the important contributions to the EOS as temperature, and thus ionization state, changes; (2) states whose energy lies somewhat below the continuum edge shift, $-\zeta_j e^2/\lambda_A$, are moved back to their isolated particle positions. This is because the λ_A dependence in the Boltzmann factors, $\exp[-\beta E_s(\lambda_A)]$ of the original expansion was used in the process of creating the new activity variables. However, states lying in the vicinity of the continuum edge are affected by plasma screening and share their degeneracy with neighboring ions [10]. The total number of states that need to be considered is nevertheless determined by the screened potential. How particular states are treated in the analysis depends on the size of the Boltzmann factors $\exp[-\beta E_s(\lambda_A)]$, where $E_s(\lambda_A)$ is the energy of states in the screened potential. For example, the degeneracy-weighted Boltzmann factor for a particular low-lying state at low temperature is $g_s \exp(-\beta E_s^0)$ until $\lambda_A \cong 1.5\lambda_c$ for that state, where E_s^0 is the atomic value and λ_c is the value of λ_A where $E_s(\lambda_A)=0$. As the density is increased further, g_s is reduced, becoming zero as $\lambda_A = \lambda_c$. Finally, a reorganization that takes advantage of the charge asymmetry when $\zeta_j > 1$ is carried out. This allows the treatment of strongly coupled, highly ionized, high-Z plasmas, provided the electron-ion coupling parameter

$$\Lambda_{ej} = \frac{\beta \zeta_j e^2}{\lambda_A} \tag{9}$$

is $\leqslant 1$, where $j = \{i\}, \{i_c\}$. The method used in the present calculations to include strong-coupling effects considers only the direct Coulomb interaction between ions. It fails when the ion core size becomes comparable to a and the core-core interactions become important [9].

The version of ACTEX used in the current calculations differs from earlier versions in one significant way, namely, the criteria used to determine the critical screening values for multielectron ions. In earlier versions, due to the complexity of calculating the states of an ion having N_b bound electrons, in which the Coulomb interaction has been replaced by the exponentially screened Coulomb potential, a scaling method based on just the tail, $(Z-N_b)e^2 \exp(-r/\lambda_A)/r$, of the self-consistent potential was used. Critical screening values for the bound states in this potential are given in Ref. [33]. However, when the number of core electrons is large, the binding is somewhat stronger and the critical value of λ_c where a state becomes unbound is lower than given by the tail part of the potential. Furthermore, as pointed out in Appendix B of Ref. [9], the electrons in a given subshell all disappear at about the same point as when only one electron occupies the shell. For high-Z ions that are not highly ionized, this can greatly reduce the critical screening length, thus causing states of ions with multiply occupied outer shells to remain bound until somewhat higher density. These considerations will mostly only affect valence shell states. The critical screening values for excited states in other shells are approximated reasonably well by the old method.

The critical screening values give the value of the screening length where the electron is no longer bound in that state to a single charge center; it does not preclude quasimolecular states where electrons are shared by several ions. The usual assumption is that the electron becomes an unbound particle free to roam throughout the system. This seems correct for excited states. However, high density is required to screen out the valence states. In this case it would seem that quasimolecular formation, where several ions share electrons for extended periods of time, are possible, i.e., the ionized electrons would not immediately wander far from their parent ions. There is some experimental evidence for this type of behavior [34]. The recent observation of high-temperature hydrogen with metalliclike properties could also be interpreted with this type of picture [35]. For plasma densities not far above where critical screening occurs, the EOS properties may not differ significantly from treating the quasimolecule as N_m distinct ions. If this is the case, then treating the valence states as atomic (isolated) states, even when $\lambda_A \cong 1.5\lambda_c$, could provide a practical method to extend the range over which reliable results are obtained. In the following we use both the screened and quasimolecular approaches, at high ρ, to obtain the valence state contributions in comparisons with experimental data. The effect of the core electrons on the critical screening value of a given shell was obtained using a quantum defect approximation to obtain an effective ζ^* to put in the scaling formula.

III. EXPERIMENTAL DATA

Ultrahigh pressure shock data have come mostly from Russian sources. These experiments have been done using underground nuclear explosives as the source of the shock wave. In a number of cases, results for experiments carried out years ago have only recently been reported. In the United States, some data have been obtained from underground nuclear explosives, and, very recently, from high-power pulsed lasers. We reviewed the available experimental data for suitable comparisons with ACTEX calculations. We looked for data on low-Z elements and compounds that were shocked to temperatures where significant ionization would be expected, and when the plasma would be in the intermediate-coupling regime. We found that D, Be, CH, H_2O, Al, and SiO_2 were the best candidates.

For D_2, there has been gas-gun shock Hugoniot data up to 200 kbar available since 1983 [36]. However, at this pressure

D_2 is only slightly dissociated, and is not yet a plasma. The very recent Nova laser experiments of Da Silva *et al.* [3] have extended the range to above 2 Mbar where dissociation is complete and some ionization has started to occur. These experiments revealed a strong density maximum in the Hugoniot due to molecular dissociation. For Be, there have been gas-gun experiments [37,38] and five data points from underground nuclear explosions [39,40].

For polystyrene, CH, there have been conventional explosive-generated shock experiments up to 0.5 Mbar [41] and recent Nova data up to 40 Mbar [42]. The Nova results are based on an x-ray contrast shadowgraph technique which is less accurate than in the D_2 experiments, and this leads to substantially larger error bars. For water the explosive and gas-gun data go up to 1 Mbar [43,44], and Russian nuclear experiments have achieved pressures up to 31 Mbar, where dissociation has occurred and partial ionization has begun [45–47]. In the case of Al, Russian nuclear explosion experiments have been taken up to 4000 Mbar, far higher than for any other material [48–51]. These data are important because they are the only published work that enters the electron shell ionization region. Additional data are available from other sources [52–53]. For silicon dioxide, there are underground nuclear explosion data [46] for several starting densities. We have chosen the starting density 1.35 g/cm^3 (one-half normal crystal density) so that the thermal effect of porosity will be optimized for comparison with ACTEX.

IV. COMPARISON OF EXPERIMENT AND THEORY

The Hugoniot curve is the locus of points attainable by shocks of increasing intensity from some fixed initial state. According to the Rankine-Hugoniot relations [54] that result from energy, momentum, and mass conservation, the internal energy at a point along the Hugoniot is given by relation

$$E_H = E_{0H} + \tfrac{1}{2}(V_{0H} - V)(P_H + P_{0H}), \tag{10}$$

where H refers to the final state and $0H$ refers to the initial state. The Hugoniot curve is determined theoretically by selecting a volume $V = M/\rho$ of interest and iterating on the temperature until the relation Eq. (10) is satisfied. In practice, as will be seen, there can be several temperatures at a given density where the EOS satisfies this condition. Since ACTEX is not valid at the cold initial state, it is necessary to use experimental data to obtain E_{0H} and V_{0H} when T_{0H} and P_{0H} are known. In most cases T_{0H} is room temperature and P_{0H} is 1 atm. Using Eq. (10) with the classical ideal gas relationship between E and P, we see that for an ideal monatomic gas of ions and electrons at infinite temperature (disregarding the presence of thermal radiation), $\rho_H = 4\rho_{0H}$. For an ideal diatomic gas, $\rho_H = 8\rho_{0H}$. Any physically correct plasma EOS model (such as ACTEX) will show the limiting shock density of $4\rho_{0H}$. However, phenomena such as dissociation and ionization will cause an increase in the molar heat capacity and a consequent increase in shock density beyond this limit. At very high temperatures, when all electrons are ionized, the density will smoothly approach the limit. Table I gives the initial values of temperature, density, and energy for the calculations discussed below.

TABLE I. Initial temperatures, densities, and energies for ACTEX Hugoniot calculations.

Material	Temperature (K)	Density (g/cm^3)	Energy (erg/g)
D_2	20	0.17	-1.089×10^{12}
Be	295	1.85	-3.55×10^{11}
CH	295	1.044	-6.42×10^{11}
H_2O	295	1.00	-5.36×10^{11}
Al	295	2.70	-1.21×10^{11}
SiO_2	295	1.35	-3.08×10^{11}

The comparison of experiment with several theories for the deuterium Hugoniot are shown in Fig. 1. The ACTEX calculations were done with the P_2 approximation described in Sec. II of Ref. [9], with the modification described above where the $1s$ ground state is not screened. We will refer to this as the P_{2uv} approximation. In the specific case of D, the plasma coupling is weak, so that screening the $1s$ state or adding the P_3 term has very little effect on the results. However, the atom-atom and atom-ion contributions to P_{2uv} are substantial and should also be included in the P_{3uv} term.

The sharp density maximum shown in the experiment is due to the large change in internal energy as D associates into D_2 molecules with decreasing T. We have not attempted to include the molecular dissociation in the ACTEX calculations and thus cannot obtain the density maximum observed in the Hugoniot data. However, ACTEX does show good agreement with the experiment in the region of the maximum. ACTEX also predicts a small secondary maximum near 10 Mbar, which corresponds to the ionization of D atoms. Further Nova experiments may be able to explore the region above 1 Mbar in more detail [55].

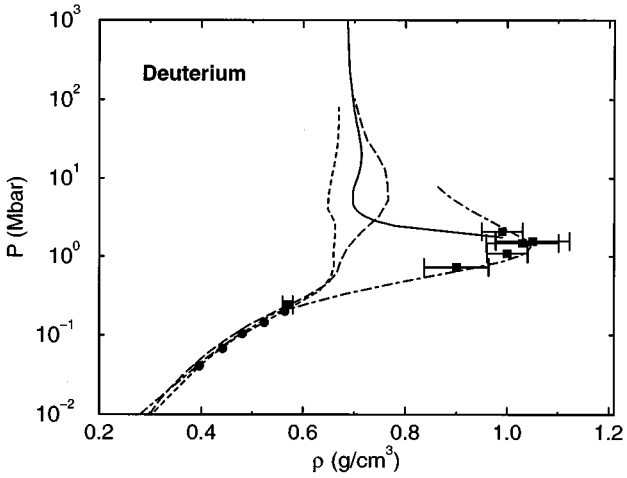

FIG. 1. Comparison of several deuterium EOS models with the experimental data (points) and ACTEX (smooth curve). The dots are gas-gun data [36] and the squares are laser data [3]. Here and in the following error bars are indicated where available. DTF (short-dashed line) is based on Thomas-Fermi theory [57], SESAME (long-dashed line) is based on an insulator-metal transition model [56], and Ross's theory (dot-dashed line) is based on liquid perturbation theory [3]. All of these theories include approximate dissociation models.

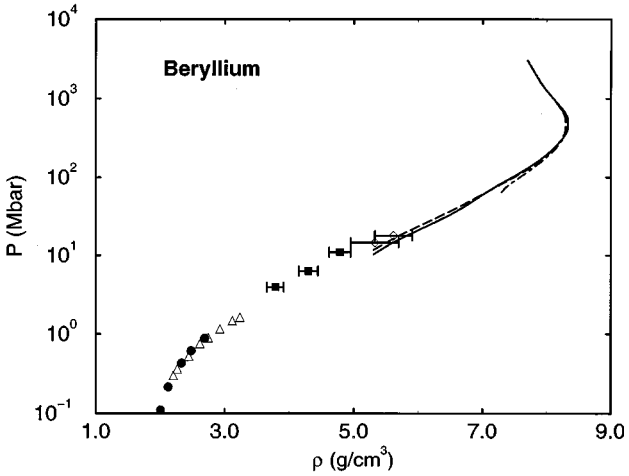

FIG. 2. Comparison of three versions of the ACTEX theory (curves; described in text) and experimental data (points) for the beryllium Hugoniot. The dots and triangles are explosive and gas-gun data [37,38], while the squares and diamonds are underground nuclear data [39,40].

The SESAME EOS includes a dissociation model with an insulator-metal transition [56]. The theory of Ross [3] uses a liquid perturbation theory with a volume-dependent dissociation energy and gives reasonable agreement with experiment. DTF [57] is a Thomas-Fermi–based theory with diatomic molecular physics added. There are substantial discrepancies between the various approaches, especially in the location of the density maximum. The DTF model overestimates the electron pressure and fails to predict any density maximum. SESAME is in poor agreement with experiment probably because of an inadequate dissociation model. Ross' model does well in the dissociation region, but only crudely treats the ionization region. It is clear that the prediction of the behavior of shocked liquid deuterium is a difficult and not yet completely solved problem.

Figure 2 shows the comparisons for Be. The ACTEX P_{2uv} (solid line) results fall slightly below the two highest experimental points. Converged solutions to the activity equations could not be obtained below 5.3 g/cm^3 and 9.8 eV. Two additional variants of ACTEX are shown. One shows that adding the P_{3uv} (dashed line) term improves the agreement with theory. In this case the core interactions are small. For the other materials discussed below, repulsive core interactions are larger and the P_{3uv} term actually slightly worsens the comparison with experiment. The other variant of ACTEX (dotted line) shows that the model that allows screening of states connected with the valence electronic configurations breaks down sooner than the P_{2uv} variant. It is evident that core interactions cannot be neglected, and so we have adopted the P_{2uv} variant as the standard calculation, which is used in the remainder of the comparisons shown.

It is useful to compare Thomas-Fermi theories with ACTEX for Be. The density maximum due to ionization occurs at $\rho = 7.74$, 7.90, and 8.35 g/cm^3 for QEOS (Thomas-Fermi) [58], SESAME (Thomas-Fermi-Dirac), and ACTEX. It is clear that the TFD model is an improvement over pure TF. Further corrections to the Thomas-Fermi model might approach the ACTEX results closely.

Figure 3 shows the ACTEX comparison with experimental polystyrene (CH) data. Predicted pressures fall below the measurements, but are within the error bars. The ACTEX calculations predict a sharp density maximum near 100 Mbar corresponding to the ionization of the $1s$ electron in H, and a broader maximum corresponding to the ionization of the $1s^2$ electrons in C. These features are an outcome of the mixture model used in ACTEX and are experimentally verifiable in principle. At densities just below those shown, the ACTEX Hugoniot curves downward and no solutions to Eq. (10) were found for $\rho < 3.4$ g/cm^3.

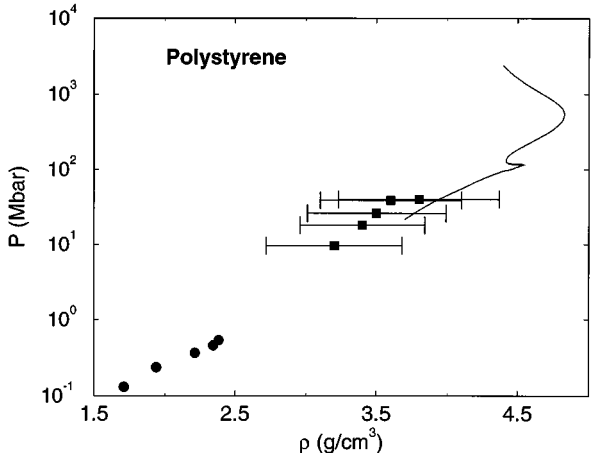

FIG. 3. Comparison of ACTEX theory (smooth curve) and experimental data (points) for the polystyrene Hugoniot. The dots are explosive data [41], and the squares are Nova laser data [42].

For water (Fig. 4) the ACTEX calculation just barely overlaps the experimental range. There is a significant change in the ACTEX slope predicted near the highest experimental points, which brings the calculations into good agreement with the data. No density oscillation due to H ionization is found in the ACTEX calculations.

For Al, the experimental data overlap the theory over the entire range considered. Here as shown in Fig. 5 the experimental data reach the electron-shell ionization region. The errors in the experiments are too large to reveal the expected ionization oscillations in the Hugoniot density, but the theory

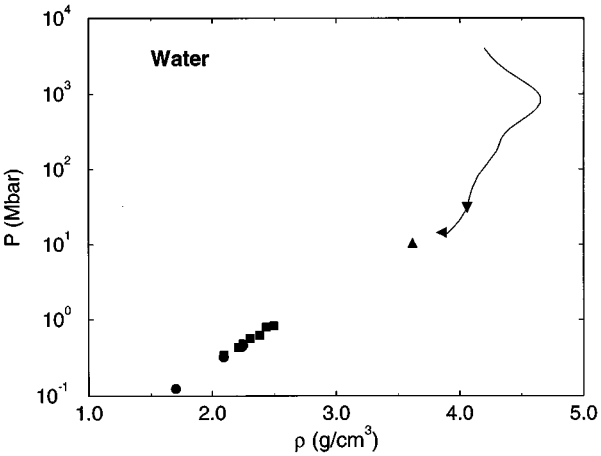

FIG. 4. Comparison of ACTEX theory (smooth curve) and experimental data (points) for the water Hugoniot. The dots and squares are explosive and gas-gun data [43,44], and the triangles are underground nuclear data [45,46].

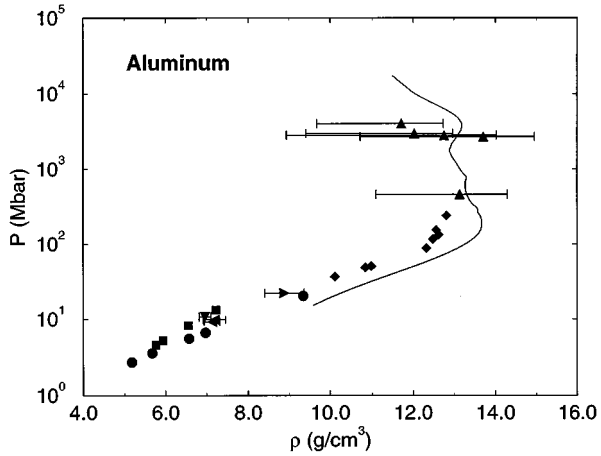

FIG. 5. Comparison of ACTEX theory (smooth curve) and nuclear explosion experimental data [47–52] (points) for the aluminum Hugoniot.

clearly indicates two major density maxima due to the ionization of the K and L electron shells. At low pressure the ACTEX slope agrees quite well with the data, but the pressure is somewhat low. This discrepancy could be explained by the neglect of hard-sphere-like interactions between M-shell ions that affect the pressure but not the energy. Various theories for shocked aluminum, including self-consistent one-electron quantum-mechanical models, have been compared for aluminum [47]. The varied results show that there is not yet a standard model that includes all of the necessary physics.

For SiO_2 (Fig. 6), the theory does not reach the highest experimental point, but the trajectory of the theory clearly points in the right direction. Ionization of the Si and O atomic cores produces some structure in the density maximum region.

The lowest-temperature points of ACTEX for the six materials are shown in Table II. It is clear that the ionic coupling given by the Γ parameter is in the transition region between weak and strong, that is, in the region where the radial distribution function begins to show oscillations due to particle correlations.

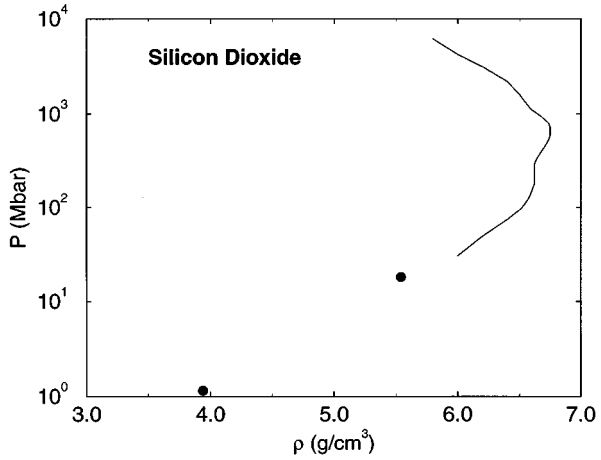

FIG. 6. Comparison of ACTEX theory (smooth curve) and nuclear explosion experimental data [46] (points) for the porous silicon dioxide Hugoniot.

TABLE II. The lowest-temperature point computed by ACTEX. The Z_m value is the charge on the most highly occupied charge state. Γ is the ion-ion coupling constant, $Z_m^2 e^2/akT$. For deuterium Z_m is the ionization fraction.

Material	Density (g/cm^3)	Temperature (eV)	Pressure (Mbar)	a (bohr)	Z_m	Γ
D	0.99	3.81	1.75	1.76	0.3	0.37
Be	5.31	9.89	10.33	1.58	2	6.96
CH	3.70	23.00	21.62	2.15	2	2.34
H_2O	3.90	13.23	13.88	1.53	2	5.30
Al	9.60	16.32	15.35	1.96	3	7.66
SiO_2	6.00	30.33	30.56	2.08	4	6.90

V. DISCUSSION

We have used nuclear explosion and laser shock data to validate the ACTEX EOS method. Overall, the ACTEX theory and experiment are in good agreement. This suggests that the ACTEX model can be used to provide the large amounts of EOS data required to model giant planets, dense stellar objects, and inertial confinement fusion (ICF) plasmas, at least for the substantial regions where conditions are similar to or less strongly coupled than those considered here. The optical properties of matter at these conditions are also an important physical input to the modeling. The ACTEX method can be used to provide the bound-state occupation numbers needed to calculate these properties [59].

We have also made comparisons with some other approaches. Thomas-Fermi–based codes like QEOS generally give reasonable values for the EOS but due to the smoothing of the shell structure will not give accurate values for derivatives of the EOS in regions of partial ionization. One indication of this is that the predicted QEOS Hugoniot density maximum is invariably lower than the ACTEX prediction. Methods that probe the interiors of giant planets and stars using seismic observations depend critically on the derivatives of the EOS [60,61], so that the Thomas-Fermi method is not applicable.

The ACTEX calculations reported here differ somewhat from earlier work in the way valence states are treated at high density. It was found that treating these states as forming quasimolecules, unaffected by plasma screening, gave significantly improved comparisons with experiment over calculations that introduce screening. An alternative explanation for this could be that the λ_A predicted by the ACTEX calculation is too short, causing valence states to be screened into the continuum at too low density. As discussed in Sec. II, higher-order terms, not included in the current calculations, cause ACTEX to become unreliable as the condensed-matter regime is approached. These terms tend to increase the value of λ_A obtained from a converged solution to the activity equations, so that allowing valence states to remain bound when $\lambda_A < \lambda_c$ may approximate the effect of including higher-order terms.

The most important improvement to ACTEX needed in the intermediate coupling region, for few-times ionized ions, is the inclusion of core-interaction terms into the P_{3uv} and possibly similar higher-order terms. There is a noticeable tendency in Figs. 2–6 for the ACTEX Hugoniot to fall below

the experimental points. This appears to be a consequence of the lack of ion-core interactions in the higher virial coefficients, since small corrections to the pressure will bring the theory into better agreement with experiment.

There is a steadily increasing interest in ultrahigh-pressure states of matter for applications such as shocked foams, laser fusion, surface ablation by x rays, meteorite and comet impacts, and planetary and stellar interior evolution. These studies require accurate tabular EOS representations over wide ranges of density and temperature, which can be accessed by hydrodynamic simulation codes. In addition, there are new experimental methods such as sonoluminescence and ultrashort pulse lasers that can generate ultrahigh-pressure states of matter under reproducible conditions and could become sources of EOS data in the future. These methods will require analysis by accurate EOS models such as ACTEX. ACTEX cannot produce a global EOS table, but it can produce partial tables for assembly into larger synthetic tables, or it can be used as quasiexperimental data to be fitted by a simpler EOS model with adjustable parameters and which can then be used to generate a global table. ACTEX appears to be a good model model for partially ionized plasmas, and will be useful for calibrating EOS data tables for simulations of processes at very high pressures and temperatures.

ACKNOWLEDGMENTS

We thank R. Cauble and W. Nellis for the release of shock data prior to publication, J. D. Johnson for SESAME data, and H. E. DeWitt for useful comments on the manuscript. This work was performed under the auspices of the U.S. Department of Energy by Lawrence Livermore National Laboratory under Contract No. W-7405-Eng-48.

[1] L. V. Al'tshuler, R. F. Trunin, K. K. Krupikov, and N. V. Panov, Usp. Fiz. Nauk **166**, 575 (1996) [Phys. Usp. **39**, 539 (1996)].
[2] A. Jayaraman, Rev. Sci. Instrum. **57**, 1013 (1986).
[3] L. B. Da Silva, P. Celliers, G. W. Collins, K. S. Budil, N. C. Holmes, T. W. Barbee, Jr., B. A. Hammel, J. D. Kilkenny, R. J. Wallace, M. Ross, R. Cauble, A. Ng, and G. Chiu, Phys. Rev. Lett. **78**, 483 (1997).
[4] E. Bohm-Vitense, *Introduction to Stellar Astrophysics* (Cambridge University Press, Cambridge, 1992).
[5] S. Goldsmith, H. E. Griem, and L. Cohen, Phys. Rev. A **30**, 2775 (1984).
[6] D. Salzmann, J. Quant. Spectrosc. Radiat. Transf. (to be published).
[7] F. J. Rogers and H. E. DeWitt, Phys. Rev. A **8**, 1061 (1973).
[8] F. J. Rogers, Phys. Rev. A **10**, 2441 (1974).
[9] F. J. Rogers, Phys. Rev. A **24**, 1531 (1981).
[10] F. J. Rogers, Astrophys. J. **310**, 723 (1986).
[11] F. J. Rogers, in *The Equation of State in Astrophysics*, edited by G. Chabrier and E. Schatzman (Cambridge Univ. Press, New York, 1994).
[12] J. N. Bahcall, M. H. Pinsonneault, S. B. Basu, and J. Christensen-Dalsgaard, Phys. Rev. Lett. **78**, 171 (1997). [The OPAL EOS in this paper refers to the same calculational method as ACTEX herein.]
[13] M. Saha, Philos. Mag. **40**, 472 (1920).
[14] D. Saumon and G. Chabrier, Phys. Rev. A **46**, 2084 (1992).
[15] D. G. Hummer and D. Mihalas, Astrophys. J. **331**, 794 (1988).
[16] D. Mihalas, W. Däppen, and D. G. Hummer, Astrophys. J. **331**, 815 (1988).
[17] H. C. Graboske, D. J. Harwood, and F. J. Rogers, Phys. Rev. **186**, 210 (1969).
[18] G. M. Harris, Phys. Rev. **133**, A427 (1964).
[19] M. McChesney, Can. J. Phys. **42**, 2473 (1964).
[20] W. Ebeling, W. D. Kraeft, and D. Kremp, *Theory of Bound States and Ionization Equilibrium in Plasmas and Solids* (Akademie-Verlag, Berlin, 1977).
[21] W. D. Kraeft, D. Kremp, W. Ebeling, and G. Ropke, *Quantum Statistics of Charged Particle Systems* (Plenum Press, New York, 1986).
[22] J. Riemann, M. Schlanges, H. E. DeWitt, and W. D. Kraeft, Contrib. Plasma Phys. (to be published).
[23] H. E. DeWitt, M. Schlanges, A. Y. Sakakura, and W. D. Kraeft, Phys. Lett. A **197**, 326 (1995).
[24] H. E. DeWitt, J. Math. Phys. **7**, 6169 (1966).
[25] A. Alastuey, F. Cornu, and A. Perez, Phys. Rev. E **49**, 1077 (1994).
[26] A. Alastuey, F. Cornu, and A. Perez, Phys. Rev. E **51**, 1725 (1995).
[27] A. Alastuey and A. Perez, Phys. Rev. E **53**, 5714 (1996).
[28] J. Christensen-Dalsgaard and W. Däppen, Astron. Astrophys. Rev. **4**, 267 (1992).
[29] M. S. Cooper and H. E. DeWitt, Phys. Rev. A **8**, 1910 (1973).
[30] T. L. Hill, *Statistical Mechanics* (McGraw-Hill, New York, 1956), Chap. 5.
[31] R. Abe, Prog. Theor. Phys. **22**, 213 (1959).
[32] W. D. Slattery, G. D. Doolen, and H. E. Dewitt, Phys. Rev. A **26**, 225 (1982).
[33] F. J. Rogers, H. C. Graboske, and D. J. Harwood, Phys. Rev. A **1**, 1577 (1970).
[34] E. Leboucher, A. Poquerusse, and P. Anglo, Phys. Rev. E **47**, 1467 (1993).
[35] S. T. Weir, A. C. Mitchell, and W. J. Nellis, Phys. Rev. Lett. **76**, 1860 (1996).
[36] W. J. Nellis, A. C. Mitchell, M. van Thiel, G. J. Devine, R. J. Trainor, and N. Brown, J. Chem. Phys. **79**, 1480 (1983).
[37] S. P. Marsh, *LASL Hugoniot Data* (University of California Press, Berkeley, 1980), pp. 21–22.
[38] W. M. Isbell, F. H. Shipman, and A. H. Jones (unpublished).
[39] W. J. Nellis, J. A. Moriarty, A. C. Mitchell, and N. C. Holmes, J. Appl. Phys. (to be published).
[40] C. E. Ragan III, Phys. Rev. A **25**, 3360 (1982).
[41] S. P. Marsh, *LASL Hugoniot Data* (University of California Press, Berkeley, 1980), p. 463–464.
[42] R. Cauble, L. B. Da Silva, T. S. Perry, D. R. Bach, K. S. Budil, P. Celliers, G. W. Collins, A. Ng, T. W. Barbee, Jr., B. A. Hammel, N. C. Holmes, J. D. Kilkenny, R. J. Wallace, G. Chiu, and N. C. Woolsey, Phys. Plasmas **4**, 1857 (1997).
[43] S. P. Marsh, *LASL Hugoniot Data* (Ref. [41]), pp. 573–574.

[44] A. C. Mitchell and W. J. Nellis, J. Chem. Phys. **76**, 6273 (1982).
[45] B. K. Vodolaga, in *Recent Trends in High Pressure Research*, edited by A. K. Singh (Oxford & IBH, New Delhi, 1992), p. 208.
[46] R. F. Trunin, Usp. Fiz. Nauk **164**, 1215 (1994) [Phys. Usp. **37**, 1123 (1994)].
[47] E. N. Avrorin, B. K. Vodolaga, N. P. Voloshin, G. V. Kovalenko, V. F. Kuropatenko, V. A. Simonenko, and B. T. Chernovolyuk, Zh. Eksp. Teor. Fiz. **93**, 613 (1987) [Sov. Phys. JETP **66**, 347 (1987)].
[48] V. A. Simonenko, N. P. Voloshin, A. S. Vladimirov, A. P. Nagibin, V. N. Nogin, V. A. Popov, V. A. Vasilenko, and Yu. A. Shoidin, Zh. Eksp. Teor. Fiz. **88**, 1452 (1985) [Sov. Phys. JETP **61**, 869 (1985)].
[49] A. P. Volkov, N. P. Voloshin, A. S. Vladimirov, N. N. Nogin, and V. A. Simonenko, Pis'ma Zh. Eksp. Teor. Fiz. **31**, 623 (1980) [JETP Lett. **31**, 588 (1980)].
[50] E. N. Avrorin, B. K. Vodolaga, N. P. Voloshin, V. F. Kuropatenko, G. V. Kovalenko, V. A. Simonenko, and B. T. Chernovolyuk, Pis'ma Zh. Eksp. Teor. Fiz. **43**, 241 (1986) [JETP Lett. **43**, 309 (1986)].
[51] A. S. Vladimirov, N. P. Voloshin, V. N. Nogin, A. V. Petrovtsev, and V. A. Simonenko, Pis'ma Zh. Eksp. Teor. Fiz. **39**, 69 (1984) [JETP Lett. **39**, 82 (1984)].
[52] L. V. Al'tshuler, N. N. Kalitkin, L. V. Kuz'mina, and B. S. Chekin, Zh. Eksp. Teor. Fiz. **72**, 317 (1977) [Sov. Phys. JETP **45**, 167 (1977)].
[53] A. C. Mitchell, W. J. Nellis, J. A. Moriarty, R. A. Heinle, N. C. Holmes, R. E. Tipton, and G. W. Repp, J. Appl. Phys. **69**, 2981 (1991).
[54] R. G. McQueen, S. P. Marsh, J. W. Taylor, J. N. Fritz, and W. J. Carter, in *High-Velocity Impact Phenomena*, edited by R. Kinslow (Academic, New York, 1970), Chap. 7.
[55] R. Cauble (private communication).
[56] G. I. Kerley (unpublished).
[57] D. A. Young and E. M. Corey, J. Appl. Phys. **78**, 3748 (1995).
[58] R. M. More, K. H. Warren, D. A. Young, and G. B. Zimmerman, Phys. Fluids **31**, 3059 (1988).
[59] C. A. Iglesias and F. J. Rogers, Astrophys. J. **339**, 717 (1996).
[60] D. O. Gough, J. W. Leibacker, P. H. Scherrer, and J. Toomre, Science **272**, 1281 (1996).
[61] B. Mosser, in *The Equation of State in Astrophysics*, edited by G. Chabrier and E. Schatzman (Cambridge University Press, New York, 1994).